Appeared in Proc. of International Conference on Pattern Recognition (ICPR), Quebec City, August 11-15, 2002.

A Hybrid Fingerprint Matcher

Arun Ross, Anil Jain
Michigan State University
East Lansing, MI, USA 48824
{rossarun, jain}@cse.msu.edu

James Reisman
Siemens Corporate Research, Inc.
Princeton, NJ, USA 08540
james.reisman@scr.siemens.com

Abstract

We describe a hybrid fingerprint matching scheme that uses both minutiae and ridge flow information to represent and match fingerprints. A set of 8 Gabor filters, whose spatial frequencies correspond to the average inter-ridge spacing in fingerprints, is used to capture the ridge strength at equally spaced orientations. A square tessellation of the filtered images is then used to construct an eight-dimensional feature map, called the ridge feature map. The ridge feature map along with the minutiae set of a fingerprint image is used for matching purposes. The genuine accept rate of the hybrid matcher is observed to be $\sim 10\%$ higher than that of a minutiae-based matcher at low false accept rates. Fingerprint verification using the hybrid matcher on a Pentium III (800 MHz) processor, takes ~ 1.4 seconds.

1. Introduction

Fingerprint matching techniques can be broadly classified as being minutiae-based or correlation-based. Minutiae-based techniques attempt to align two sets of minutiae points and determine the total number of matched minutiae [6]. Correlation-based techniques, on the other hand, compare the global pattern of ridges and furrows to see if the ridges in the two fingerprints align [1]. The performance of minutiae-based techniques relies on the accurate detection of minutiae points and the use of sophisticated matching techniques to compare two minutiae fields which undergo non-rigid transformations. The performance of correlation-based techniques is affected by non-linear distortions and noise present in the image. In general, it has been observed that minutiae-based techniques perform better than correlation-based ones.

Jain *et al.* [5] have proposed a novel representation scheme that captures global and local features of a fingerprint in a compact fixed length feature vector, called the *FingerCode*. This technique views a fingerprint as an oriented texture (Figure 1) and their generic representation of

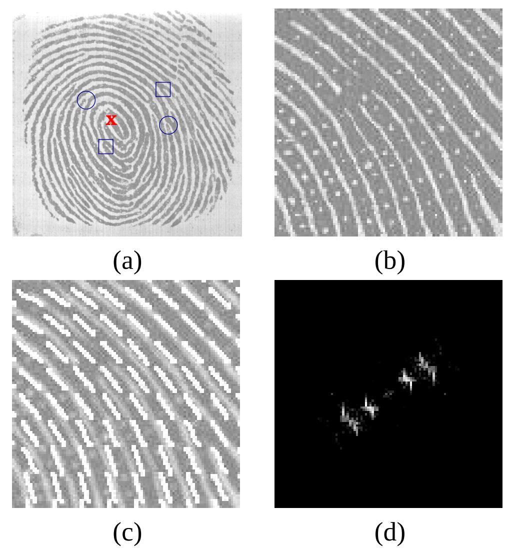

Figure 1. Fingerprint as an oriented texture pattern. (a) A fingerprint with the core ($\times$) and four minutiae points (ridge ending - $\circ$; ridge bifurcation - $\square$) marked on it; (b) the constant inter-ridge spacing in a local region of the fingerprint; (c) the dominant direction of the ridges in (b); (d) the power spectrum of (b).

oriented texture relies on extracting a core point in the fingerprint. Their technique, however, suffers from the following shortcomings: (i) The frame of reference is based on a global singular point i.e., the core point (Figure 2(a)). Detection of the core point is non-trivial; the core point may not even be present in small-sized images obtained using solid-state sensors. (ii) The fingerprint alignment is based on a single reference point and is, therefore, not very robust with respect to errors in the location of the reference point. (iii) The tessellation does not cover the entire image. Furthermore, if the core were to be detected close to the boundary of the image, the tessellation will include an extremely small portion of the image.

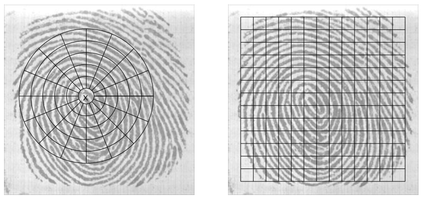

(a) (b)

Figure 2. Tessellating the fingerprint image. (a) Circular tessellation (80 $sectors$) about a core point. (b) Square tessellation (169 $cells$) over the entire image.

We present a fingerprint representation scheme that constructs a ridge feature map by observing the local ridge orientation. The local ridge characteristics are extracted via a set of Gabor filters whose frequency corresponds to the inter-ridge spacing in fingerprints. Unlike in [5], the filtering is done on the enhanced images rather than the raw input images. Instead of using circular tessellation, a square tessellation is used (Figure 2(b)). The tessellation includes the entire image, and all the tessellated cells are of the same size. The tessellation is not based on detecting any landmark points. The fingerprint images are aligned using the overall minutiae information; this is more robust than using only the core point for aligning image pairs as done in [5].

2. Ridge Feature Maps

By tuning a Gabor filter to a specific frequency and direction, texture information from images can be extracted [2]. An even symmetric Gabor filter has the following general form in the spatial domain:

$$G_{\theta,f}(x,y) \;=\; exp\left\{\frac{-1}{2}\left[\frac{x'^2}{\delta_x^2}+\frac{y'^2}{\delta_y^2}\right]\right\}cos(2\pi f x'),$$

$$x' = xsin\theta + ycos\theta, y' = xcos\theta - ysin\theta,$$

where f is the frequency of the sinusoidal plane wave at an angle θ with the x-axis, and δ_x and δ_y are the standard deviations of the Gaussian envelope along the x and y axes, respectively. For the 240×240 images obtained using the Veridicom sensor (see section 4), the Gabor parameters are set to the following values: (i) f = 0.125 (corresponds to an inter-ridge distance of 8); (ii) δ_x = δ_y = δ = 4 (based on empirical data); (iii) $\theta = \{0°, 22.5°, 45°, 67.5°, 90°, 112.5°, 135°, 157.5°\}$, resulting in eight Gabor filters.

(a) (b)

Figure 3. Fingerprint image (a) before and (b) after enhancement.

We enhance the input image [3] prior to filtering (in order to improve the clarity of ridges and furrows). The minutiae features are also extracted after processing the enhanced fingerprint image. Figure 3 shows a fingerprint image before and after enhancement. Filtering requires convolving the enhanced image with each of the 8 Gabor filters in the spatial domain. In order to speed-up the filtering, the convolution is performed in the frequency domain. Eight filtered images are obtained as a result of this filtering (Figure 4).

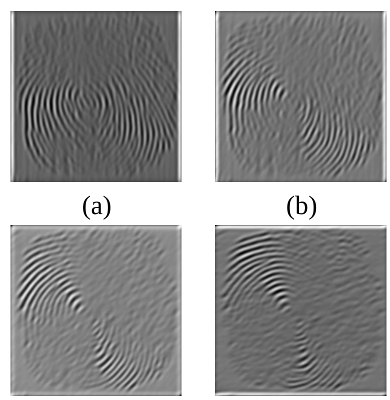

(a) (b) (c) (d)

Figure 4. Filtering of the image in Figure 3(b). Only 4 of the 8 filtered images are shown.

While a filtered image in its entirety can be used as a representation scheme, the presence of local distortions would affect the matching process drastically. Moreover, it is the local variations in ridge structure (combined with the global ridge configuration) that will provide a better representation of the fingerprint. To examine local variations, the image is tessellated into square cells, and features from each of the cells are computed. The size of a cell is chosen to correspond to twice the inter-ridge spacing (16×16). A 16-pixel wide border of the image is not included in the tessellation. This results in $n_c = 13$ cells in each row and column of the square grid, with a total of 169 cells. The *variance* of the pixel intensities in each cell of all 8 filtered images is used as a feature vector. The variance corresponds to the energy of the filter response, and is, therefore, a useful measure of ridge orientation in a local neighborhood. Those tessellated cells that contain a certain proportion of background pixels are labeled as background cells and the corresponding feature value is set to zero. An eight-dimensional feature map (13×13 image) corresponding to the 8 filtered images is obtained in this way (Figure 5). These ridge feature maps are used to represent and match a query image with a template.

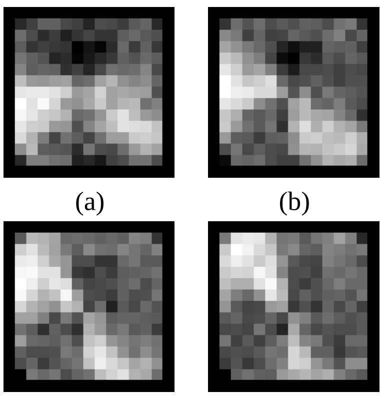

(a) (b) (c) (d)

Figure 5. Feature maps (13×13 images) for the 4 filtered images in figure 4.

3. Hybrid Fingerprint Matcher

The hybrid fingerprint matcher proposed here utilizes two distinct sets of fingerprint information: minutiae features, and ridge feature maps. Minutiae information is obtained using the technique described in [4]. When a query image is presented, the matching proceeds as follows: (i) the query and template minutiae features are matched to generate a minutiae matching score *and* an affine transformation that aligns the query and template fingerprints; (ii) the query image is filtered using 8 Gabor filters; (iii) the ridge feature map is extracted from these filtered images; (iv) the query and template ridge feature maps are matched; (v) the minutiae and ridge feature map matching scores are combined to generate a single matching score (Figure 6).

For comparing the ridge feature maps of two images, it is necessary that the images themselves are aligned appropriately to ensure an overlap of common region in the two fingerprint images. This is done by determining the affine transformation parameters, (t_x, t_y, t_ϕ), that would align the query image with the template. The transformation parameters are computed by matching the two sets of minutiae points using an elastic point matching algorithm [4]. Instead of rotating the query image by t_ϕ and then filtering it, the Gabor filters are appropriately rotated and the *modified* Gabor filter bank is applied to the query image. The resulting filtered images are then rotated by t_ϕ and translated by (t_x, t_y). This reduces the artifacts associated with filtering a rotated image.

The minutiae matching score is a measure of the similarity of the minutiae sets of the query and template images. The similarity score is normalized in the $[0, 100]$ range. The ridge feature maps of the query and the template images are compared by computing the sum of the Euclidean distances of the 8-dimensional feature vectors in the corresponding tessellated cells. (Cells that are marked as background, are not used in the matching process). The distance score is normalized in the $[0, 100]$ range, and converted to a similarity score by simply subtracting it from 100. Let S_M and S_R indicate the similarity scores obtained using minutiae matching and ridge feature map matching, respectively. Then, the final matching score, S, is computed as, $S = \alpha S_M + (1 - \alpha) S_R$, where $\alpha \in [0, 1]$. For the experimental results reported in this paper, α was set to 0.5.

4. Experiments and Results

The fingerprint database used in our experiments consists of fingerprint impressions obtained from 160 non-habituated, cooperative subjects using the Veridicom sensor (300×300 images at 500 dpi). The data was collected over two sessions. In each of the sessions, a subject was asked to provide 2 impressions of each of 4 different fingers - the left index finger, the left middle finger, the right index finger and the right middle finger. A total of $2,560$ images were acquired over two time sessions. This is a difficult database for a fingerprint matcher due to the following reasons: (i) The small-sized sensor captures only a limited portion of the subject's fingerprint, and multiple impressions of the same finger, in some cases, had very little overlap. (ii) Many subjects were observed to have dry fingers that resulted in partial or faint prints. The 300×300 images were first resized to 240×240 (inter-ridge distance was reduced from 10 pixels to 8 pixels), and then padded with zeros to expand them to 256×256, in order to speed-up the Fourier operations. The ROC (Receiver Operating Characteristic) curves depicting the performances of the minutiae, ridge feature map and hybrid matchers are shown in Figure 7. The hybrid technique outperforms the minutiae-based scheme over a wide range of FAR values. The equal error rate of the hybrid technique is observed to be $\sim 4.5\%$, while that of the minutiae-based matcher is $\sim 14\%$. The experiments also show that the minutiae information and ridge flow information complement each other.

The experiments reported here were conducted on a Pen-

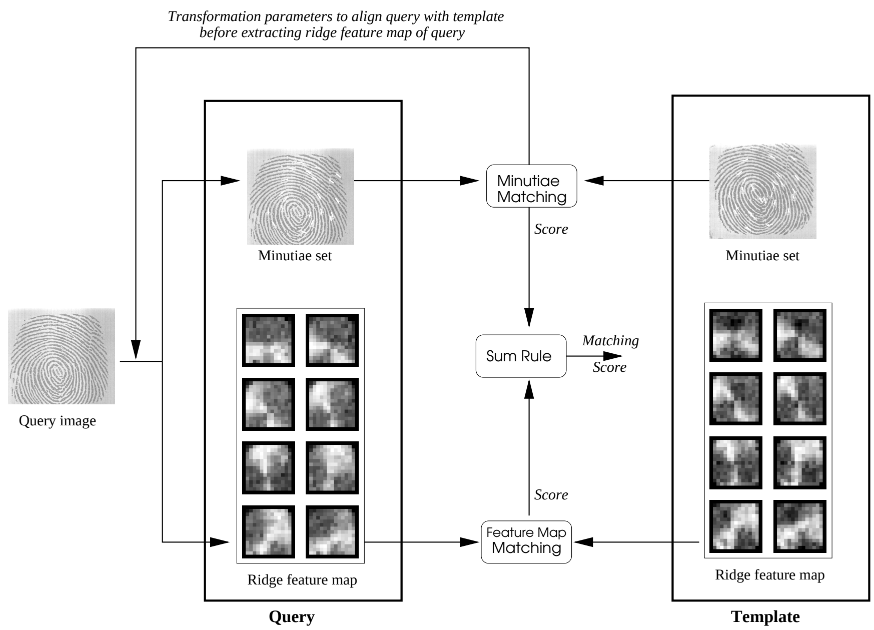

Figure 6. The matching process.

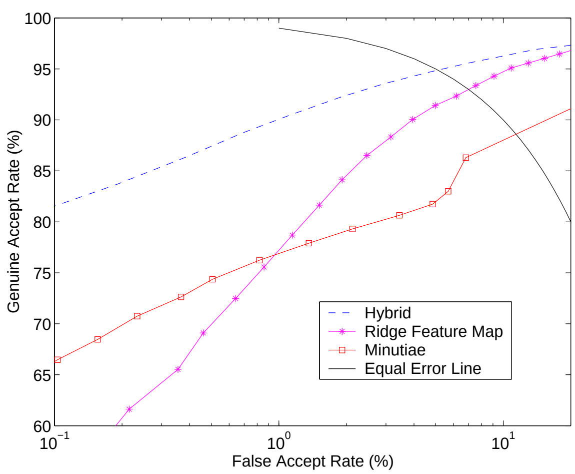

Figure 7. ROC showing the performances of the three matchers.

tium III, 800 Mhz processor, running Windows 2000. The total time for fingerprint verification (one-to-one matching) was ~ 1.4 seconds.

5. Summary and Future Work

We have proposed a fingerprint matching technique that combines minutiae information with the ridge flow information. Experiments indicate that the hybrid technique performs much better than a purely minutiae-based matching scheme. Currently, the minutiae information is used to align the query and the template images, before computing the ridge feature map. We are working on non-minutiae based alignment techniques that make use of orientation field and ridge map information to align image pairs.

References

[1] A. M. Bazen, G. T. B. Verwaaijen, S. H. Gerez, L. P. J. Veelenturf, and B. J. van der Zwaag. A correlation-based fingerprint verification system. In *Proceedings of the ProRISC2000 Workshop on Circuits, Systems and Signal Processing*, Veldhoven, Netherlands, Nov 2000.

[2] J. Daugman. Recognizing persons by their iris patterns. In A. K. Jain, R. Bolle, and S. Pankanti, editors, *Biometrics: Personal Identification in a Networked Society*, pages 103–121. Kluwer Academic Publishers, 1999.

[3] L. Hong, Y. Wan, and A. K. Jain. Fingerprint image enhancement: Algorithms and performance evaluation. *IEEE Transactions on PAMI*, 20(8):777–789, Aug 1998.

[4] A. K. Jain, L. Hong, and R. Bolle. On-line fingerprint verification. *IEEE Transactions on PAMI*, 19(4):302–314, April 1997.

[5] A. K. Jain, S. Prabhakar, L. Hong, and S. Pankanti. Filterbank-based fingerprint matching. *IEEE Transactions on Image Processing*, 9(5):846–859, May 2000.

[6] L. O'Gorman. Fingerprint verification. In A. K. Jain, R. Bolle, and S. Pankanti, editors, *Biometrics: Personal Identification in a Networked Society*, pages 43–64. Kluwer Academic Publishers, 1999.